Contract No:

This document was prepared in conjunction with work accomplished under Contract No. DE-AC09-08SR22470 with the U.S. Department of Energy (DOE) Office of Environmental Management (EM).

Disclaimer:

This work was prepared under an agreement with and funded by the U.S. Government. Neither the U. S. Government or its employees, nor any of its contractors, subcontractors or their employees, makes any express or implied:

1) warranty or assumes any legal liability for the accuracy, completeness, or for the use or results of such use of any information, product, or process disclosed; or
2) representation that such use or results of such use would not infringe privately owned rights; or
3) endorsement or recommendation of any specifically identified commercial product, process, or service.

Any views and opinions of authors expressed in this work do not necessarily state or reflect those of the United States Government, or its contractors, or subcontractors.

NANOCOMPOSITE PHOTOCATALYSTS: CONVERSION OF CO_2 TO FUEL

Simona E. Hunyadi Murph,[1] Henry Sessions,[1]*
Yao Kun,[2] Yiping Zhao[2]

[1]Savannah River National Laboratory
National Security Directorate
Savannah River Site, Aiken, SC 29808

[2]Department of Physics and Astronomy,
and Nanoscale Science and Engineering Center,
University of Georgia, Athens, Georgia 30602

*Corresponding author e-mail: Simona.Murph@srnl.doe.gov

Abstract

Solar conversion of carbon dioxide and water vapor to carbon monoxide, hydrogen and hydrocarbons are demonstrated by exposure of titania-based nanophotocatlysts under ambient light only. TiO_2 and WO_3-core TiO_2-shell nanorod arrays fabricated by glancing angle deposition are functionalized with quantum dots (CdSe) prepared by solution chemistry. These nanocomposite structures are used as the photocatalysts for CO_2 conversion under sunlight illumination. A gas chromatographic analysis shows that the primary products are carbon monoxide, hydrogen and hydrocarbons (methanol and methane) after several hours of exposure to sun light. The overall CO_2 conversion efficiency of such core-shell and quantum dot-titania nanostructures is significantly higher than that of pure TiO_2 nanorod array photocatalyst. The improved conversion efficiency may result from the additional absorbance of visible light by WO_3 and quantum dots and the charge separation at the WO_3-TiO_2 and CdSe-TiO_2 interfaces. The conversion efficiency of such an artificial photosynthesis process remains to be improved for practical applications.

Introduction

Conversion of solar energy and waste chemicals, such as CO_2, into stored chemical energy, such as hydrocarbons, is arguably one of the most promising and environmentally friendly technologies for energy generation. A small fraction of the solar energy, if converted and stored, can significantly address the world's increasing energy needs and reduce reliance on fossil fuels and, hence, enhance America's energy security. As an added benefit, this conversion process utilizes the greenhouse gas CO_2 as a reactant making the process nearly (minus materials transport and catalyst manufacturing) CO_2 neutral.

The CO_2 conversion approach can be summarized as:[i]

$$CO_2 + H_2O + h\nu \text{ (solar light)} \rightarrow CH_4 + O_2 \quad \text{(Eq.1)}$$

However, solar light alone cannot drive the reaction. This conversion can be achieved with the help of photocatalysts. The scientific literature has produced a great amount of experiment and theory on CO_2 conversion on metal oxides, semiconductor materials or other classes.[i] However, their limitations in terms of the requirement for UV excitation and/or generally low conversion efficiencies (0.5%) have become evident. This is because reduction of CO_2 to hydrocarbons is a complex multistep reaction involving shared intermediates and multiple reaction pathways. Additionally, most of the photocatalysts have a very narrow band edge absorbance, and provide limited amount of free electrons and protons on the surface for such a reaction. Thus, to improve the CO_2 conversion efficiency, the challenge is to design a better photocatalyst that can absorb a broader spectrum of sun light and convert them more effectively to free electron-hole pair for the above reaction.

Titania has been considered the most appropriate candidate for photocatalytic processes due to its powerful oxidation capability, superior charge transport, and corrosion resistance. Additionally, TiO2 is inexpensive, has reasonable activity, and is abundant. The absorption of photons from natural light in photocatalytic materials generates electrons and holes which could drive energy conversion processes in the solar-driven photoreduction of CO_2 and/or water-splitting for hydrogen fuels. Despite these attributes, the efficiency of TiO2 for photovoltaic and photocatalytic applications is severely limited by its large band gap (~3.2 eV) and rapid charge carrier recombination dynamics which means that titania can use less than approximately 1% of the solar spectrum.[ii,iii]

We have developed and amassed a library of inexpensive, abundant and active titania based nanohybrid catalysts with multifunctional, broadband electromagnetic response for efficient solar energy conversion of CO_2 to carbon monoxide, hydrogen, methanol and methane by a combination of solution chemistries and glancing angle deposition (GLAD) approaches. We engineer the bandgap of the TiO_2 photocatalytic materials quantum dots (CdSe) and oxides (WO_3) sensitizers to maximize the reaction channels for the photocatalytic conversion. Photocatalytic conversion of CO_2 is monitored with an in-house designed chamber that allows evaluation of nanocatalysts for solar fuels applications. A gas chromatographic analysis shows that the primary product is carbon monoxide and hydrogen along with methanol and methane after several hours' exposure to sun light.

Experimental

The TiO_2 and WO_3-TiO_2 core–shell nanorod array was fabricated in a custom-built electron beam evaporation system (Torr International, New Windsor, NY).[iv] The source materials used to deposit were TiO_2 (99.9%, Kurt J. Lesker) and WO_3 (99.8%, Alfa Aesar) with no other gases present in the chamber during depositions, and the chamber background pressure was at $1–2 \times 10^{-6}$ Torr. Si wafers and glass microscope slides were both used as substrates for different characterizations techniques. The deposition thickness and rate were both monitored by a quartz crystal microbalance (QCM) facing the vapor flux direction directly. The core–shell structure was fabricated through two consecutive GLAD depositions of different materials at different incident angles as described before.[ii,iii]

All of the quantum dots were grown onto substrates of TiO_2 and that were nominally $1cm^2$ (10mm x10 mm) glass or silicon pads. The quantum dots were grown from aqueous solutions using conditions that would produce the desired deposit size and shape. Quantum dots CdSe nanoparticles were prepared by a citrate reduction approach in the presence of the ordered arrays of titania based nanorods.[v,vi] To 45 mL of water were added 0.05 g of sodium citrate (Aldrich) and 2 mL of 4 × 10-2 M cadmium perchlorate (Aldrich), and the pH was adjusted to 9.0 with 0.1 M NaOH. After the solution had been bubbled with nitrogen for 10 min, 2 mL of 1 × 10-2 M N,N-dimethylselenourea (Aldrich) was added, and the mixture was heated in a conventional 900-W microwave oven for 50 s. All samples were characterized using electron microscopy analysis (transmission electron microscopy analysis and scanning electron microscopy (SEM), particle size distribution by dynamic light scattering (DLS), zeta potential (effective surface charge) analysis, and elemental composition by energy dispersive X-ray (EDX) mapping to elucidate their morphology, topography and composition. The nanoparticle's optical properties were evaluated by UV-Vis absorption spectroscopy and photoluminescence spectroscopy.

Photocatalytic conversion of CO_2 was monitored with an in-house designed solar-gas chambers equipped with gas inlet and outlet, optical window and sample stage holder that allowed evaluation of nanocatalysts for solar fuels applications. The type and amount of hydrocarbons and other gases generated through prolonged light-soaking was quantified by both residual gas analyzis and a gas-chromatography. The retention time was measured from the time of injection to the time of maximum per deflection for the component being observed. The syringe-type chamber used was strategically selected, allowing a direct gas analysis with the micro gas-chromatograph.), without the need of intermediary sampling steps. Approximately, 1 cm3 of gas was injected each time. Standard gases were used as control samples to accurately elucidate the peak composition. Each column was calibrated before running samples of interests. The quantitative analysis of the chromatograms produced was resolved by measuring the peak area (computer generated data) of eluted compounds. The peak area is proportional to the amount (moles) of compound eluted and was expressed as abundance throughout the manuscript.

Electronic absorption spectra were acquired with a CARY 500 Scan UV–vis spectrophotometer. Photoluminescence spectra were acquired with an SLM-Aminco 8100 or a Fluoromax-3 spectrofluorometer from Jobin Yovan, with excitation at 355 nm and 4 nm slit widths. Transmission electron microscopy was performed on a Hitachi H 8000 instrument on copper grids. Scanning electron microscopy analysis was conducted on a Hitachi 4800 instrument. Light scattering and zeta potential measurements were carried out on Brookhaven Zeta PALS instrument.

Results and Discussions

Efforts have been devoted to producing and sensitizing TiO_2 nanomaterials with nanoparticles that absorb light at lower photon energies, thus extending absorption into the visible light region of the spectrum. Coupling of pure TiO_2 with quantum dots (QDs), noble metals (NPs), and other oxides (WO_3) extends the adsorption of solar energy in visible region and generate more electron-hole pairs, due to the smaller band gap of those sensitizers. This results in higher photocatalytic efficiency for the CO2 conversion process.[vii,viii]

Quantum dots (QDs) are semiconductor nanoparticles that have a diameter in the 1-10 nm range, coincident with their respective excitonic Bohr radii.[vi] Semiconductor quantum dots exhibit quantization effects in photo-conversion devices and offer several unique and important properties that are advantageous: absorption and emission spectra that can be tuned by varying size, shape, structure, or by adjusting the nature of adsorbates; preparation, surface modification, and attachment through solution-based chemistries, which are cost-saving techniques and amenable for scale up; QDs utilize multiple exciton generation and hot carriers, which can greatly improve the device applications. These materials are highly photoluminescent, resistant to photobleaching compared to organic fluorophores and their bandgap energies are exquisitely tunable with particle diameter, based on quantum confinement effects. CdSe possess bulk bandgap energies in the visible region of the electromagnetic spectrum; and the particle size in the 1-10 nm regimes tunes the bandgap energies, and thus light emission energies, to shorter wavelength compared to the bulk.[v,vi]

The TiO_2 and WO_3/TiO_2 core–shell nanorod arrays were fabricated in a unique custom-built two source electron beam evaporation system.[ii,iii] By using two consecutive glancing angle depositions (GLAD) at different deposition angles and with different materials, a WO_3-core TiO_2-shell nanostructure has been fabricated.[ii,iii] GLAD is a nanofabrication technique that has shown the ability to create uniform aligned arrays of vertical nanorods from numerous materials. This technique is based on physical vapor deposition and shadowing effect by positioning the substrate normal at a very large angle (70°C) with respect to the incident vapor direction. The as-prepared materials were annealed at different temperature to alter the crystalline structures of each component. This versatile method allows for controlled growth of both the WO_3 "core" as well as the TiO2 "shell", which maximizes the interfacial area between the two materials, but also optimizes the area of TiO_2 that is in contact with the solution. The photocatalytic enhancement of these core-shell novel structures was reported earlier to be up to 70 times over amorphous single layer TiO_2 thin films, 13 times enhancement over crystalline (anatase) TiO_2 thin films, and 3 times enhancement over c-TiO_2/a-WO_3 two-layer thin films, with much less (85%less) the load of TiO_2.[ii,iii] These structures also show strong white light responses. Since these materials shows superior photocatalytic properties were further tested as CO_2 convertors.

Cadmium selenide nanoparticles of approximatively 5 nm in diameter are prepared and characterized by electronic absorption spectroscopy and transmission electron microscopy. (Figure 1a, b). The UV–vis spectra present a typical shoulder at around 500 nm while the emission spectra display the characteristic peak at approximately 580 nm (Figure 2) which is in agreement with the size of the nanoparticles (5nm in diameter) and data reported earlier. [v,vi]

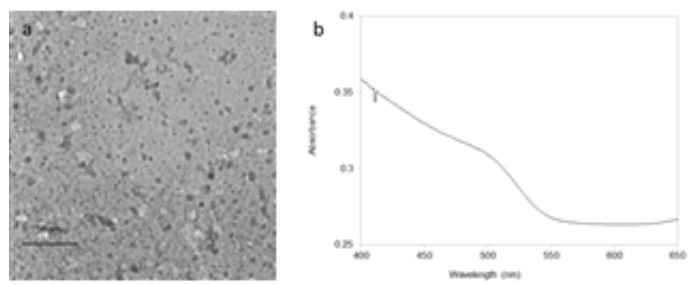

Figure 1. (a) Transmission electron micrograph of 5 nm diameter CdSe nanoparticles and (b) UV–vis spectrum. Scale bar = 50 nm.

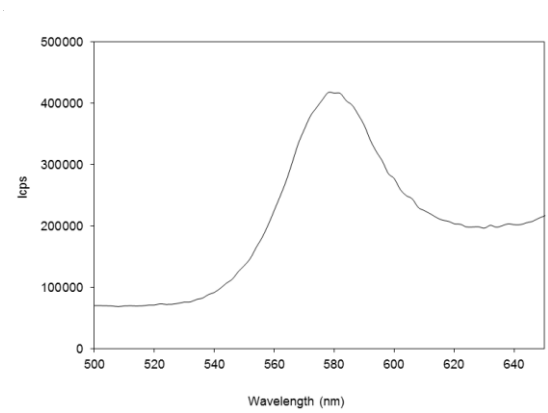

Figure 2. Emission spectra of CdSe nanoparticles excited at 355 nm.

Consistent with the implications of UV–Vis spectra, particle size analysis shows that the average CdSe particle size was 7nm (hydrodynamic radius) while the surface charge ξ= - 62±3 mV. The negative surface charge is due to the adsorbed citrate on the CdSe surface.[v,vi]

CdSe quantum dots are grown onto TiO_2 and WO_3-TiO_2 using the described procedures. The CdSe as-deposited condition of the

pad is shown in Figure 3. SEM images show that the CdSe quantum dots are uniformly distributed over the entire titania based nanorod surfaces. The UV–vis spectra show the typical absorption peaks for TiO2 around 350 nm and WO3 around 450 nm. The shoulder peak at approximately 500 nm is attributed to the CdSe nanoparticles.

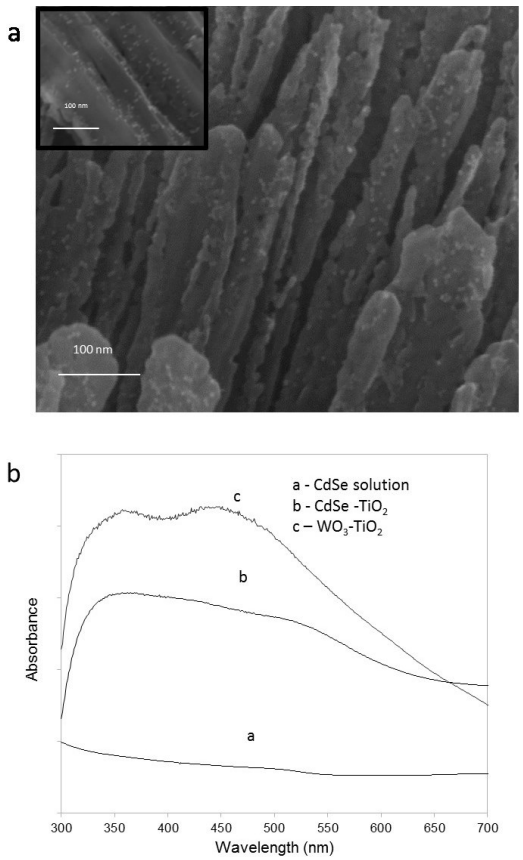

Figure 3. (a) Scanning electron micrograph of representative CdSe-WO_3-TiO_2 nanoparticles and (b) UV–vis spectrum of CdSe-TiO_2, CdSe in solution and WO_3-TiO_2. Scale bar = 100 nm.

Energy dispersive X-ray analysis (EDX) of the nanomaterials is performed to evaluate nanomaterial composition with representative data presented in Figure 4. The results reveal the presence of the main components, including Cd, Se, Ti and O. The results are in agreement with emission experiments and confirm once again the CdSe deposition on titania based ordered arrays of nanostructures.

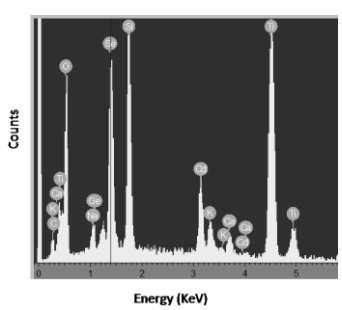

Figure 4. EDX- Semiquantitative analysis of ordered arrays of CdSe-TiO_2 nanotructures deposited on glass pads.

Nanophotocatalysts have been evaluated for photocatalytic reduction of CO_2 with H_2O vapor by exposing three 1cm^2 of catalyst in ~20 cc gas mixture and under ambient light, UV and/or UV-visible illumination. The amount of hydrocarbons as well as the kinds of hydrocarbons generated through prolonged light-soaking is quantified by gas-chromatography and/or residual gas analysis. A gas chromatographic analysis shows that the primary products are hydrogen, carbon monoxide along with hydrocarbons such as methane and methanol after several hours of exposure to sun light. Product formation rate increases with temperature and stabilized at ~35°C.

Data generated after several hours of exposure in saturated CO_2 and H_2O, on TiO_2-based nanophotocatalysts under UV and UV-Vis exposure, shows generation of hydrogen gas as depicted by residual gas analyzer (RGA) system (Figure 5a). Hydrogen generation is also confirmed by GC analysis (Figure 5b).

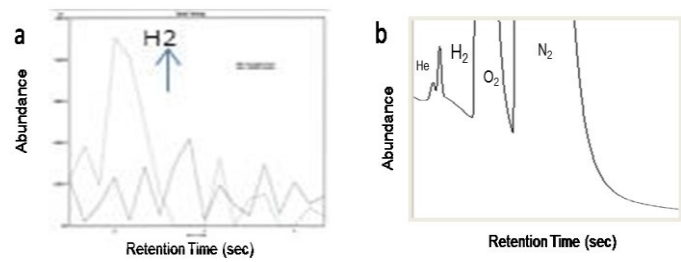

Figure 5. (a) RGA and (b) GC analysis showing H2 evolution on ordered arrays of titania based nanostructures.

Various yields of hydrogen are obtained depending on the catalysts composition and illumination conditions. Hydrogen production is found much more effective on WO_3-TiO_2 than TiO_2 when exposed under UV-Vis illumination conditions. Hydrogen production doubled on WO3-TiO2 vs. TiO2 under sun illumination. This is not surprising since under visible illumination, TiO2 cannot be activated due to its large band gap.

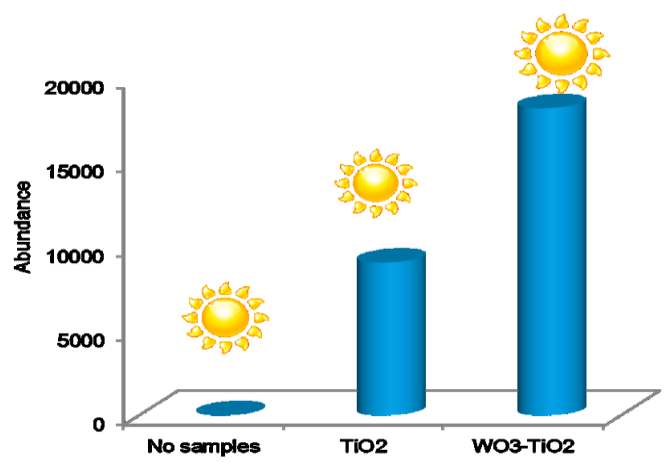

Figure 6. Hydrogen generation data collected on a micro GC in the presence of TiO_2 and/or WO_3-TiO_2 active nanophotocatalyst. TiO_2 is active only in the UV region of the spectrum, while WO_3-TiO_2 is active in UV-Vis region. H_2 production doubled under visible illumination when WO_3-TiO_2 photocatalyst was used vs. TiO_2 photocatalyst.

Evolution of hydrocarbons after prolonged light exposure detected and quantified by GC shows that a longer exposure (from 1, 4 to 8 hours) generally increases the amount of gases produced (data not shown). The amount and the type of gases produced are highly dependent upon nanoparticles' composition. Several products are detected including carbon monoxide, methanol and methane. Representative chromatographs collected on a micro-GC are depicted in Figure 7.

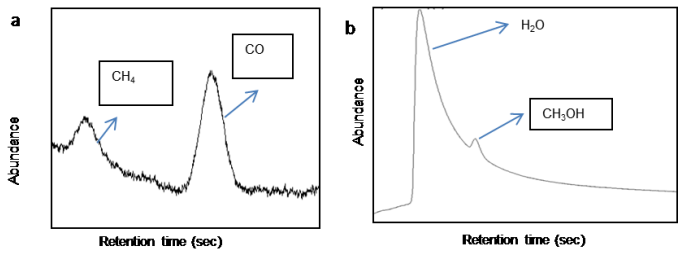

Figure 7. Chromatographs collected on a micro-GC showing carbon monoxide, methanol and methane evolution on ordered arrays of nanophotocatalysts exposed under visible illumination. GC was equipped with OV1 and pora-plot columns. OV1 for monitoring methanol and the pora plot for all other gases including H_2, CO and methane.

There are several major findings from the data collected on the GC. First, carbon monoxide production is more effective on the CdSe-TiO_2 and TiO_2 after four hours exposure under visible illumination at 35°C (Figure 8). Surprisingly, the amount of carbon monoxide evolved on the TiO_2 is three orders of magnitude higher than on WO_3-TiO_2. More experiments are underway to completely elucidate this phenomenon and will be reported at a later date.

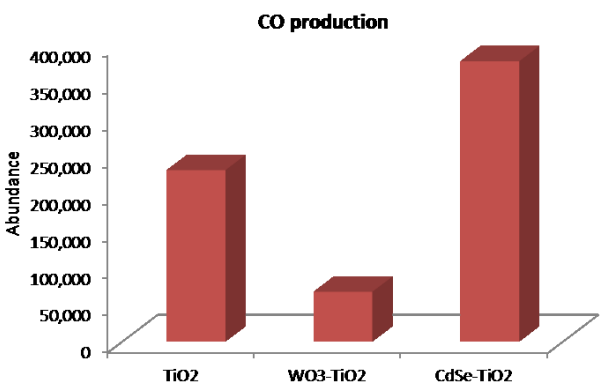

Figure 8. Carbon monoxide evolution after exposure of titania based catalysts for 4 hours at 35°C.

Numerous studies have shown that the product selectivity is highly dependent on catalyst materials.[viii,ix,x] Yu et. al[ix] demonstrated that CO_2 is reduced to CO and O_2 using Pt/TiO_2 catalysts. Varghese et al.[x] hypothesized that the photocatalytic reduction of CO_2 by Cu or Pt TiO_2 catalysts:

$$CO_2 + 2e^- + 2H^+ \rightarrow CO + \tfrac{1}{2} O_2 \quad (2)$$
$$H_2O + 2h^+ \rightarrow \tfrac{1}{2} O_2 + 2H^+ \quad (3)$$
$$CO_2(aq.) + 2H^+ + 2e^- \rightarrow HCOOH \quad (4)$$
$$HCOOH + 2H^+ + 2e^- \rightarrow HCHO + H_2O \quad (5)$$
$$HCHO + 2H+ + 2e^- \rightarrow CH_3OH \quad (6)$$
$$CH_3OH + 2H^+ + 2e- \rightarrow CH_4 + H_2O \quad (7)$$

Conversion of CO_2 to methane is a complex and multistep process: [vi,viii,ix,x xi]

$$CO_2 + H^+ + e^- \rightarrow HCO_2(ads) \quad (8)$$
$$HCO_2(ads) + H^+ + e^- \rightarrow CO + H_2O \quad (9)$$
$$2H_2O + 2h^+ \rightarrow 2OH(ads) + 2H^+ \quad (10)$$
$$2OH(ads) \rightarrow 1/2O_2 + H_2O \quad (11)$$
$$H2O + h^+ \rightarrow OH^\bullet + H^+ \quad (12)$$
$$2CO_2 + 4e^- + 4h^+ \rightarrow 2CO + O_2 \quad (13)$$
$$CO + 6e^- + 6H^+ \rightarrow CH_4 + H_2O \quad (14)$$

Methanol is favorably produced on all titania based catalysts. However, methane is detected only in the presence of WO_3-TiO_2 nanophotocatalysts. Comparison of MeOH and methane evolution over titania based catalysts are shown in Figure 9. The yield of methanol is significantly higher on CdSe-TiO_2 than either WO_3-TiO_2 or TiO_2 nanorod catalyst array. The amount of MeOH produced is doubled for WO_3-TiO_2 vs. TiO2 ordered arrays catalyst.

These results are in agreement with previous studies that suggest a higher efficiency in CO_2 photoreduction due to significantly increased lifetime of the charge-separated state.[ii, iii, vii-xi] Since the electron-hole recombination is two-three orders of magnitude faster than other electron-hole recombination any process that inhibits electron–hole recombination greatly increases the efficiency and rates of CO_2 photoreduction.[vii] Coupling the ordered TiO_2 nanorod arrays with WO_3 or CdSe nanoparticles increases spatial separation and diffusion lengths of photoexcited electrons and holes which result in increased CO_2 conversion. This indicates that the composition and ordered spatial arrangement of the TiO2 surface is an extremely important factor in its catalytic activity.[xii]

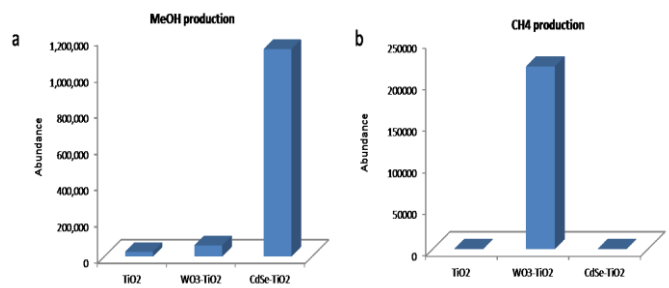

Figure 9. MeOH and CH_4 evolution on titania based catalysts.

Carbon dioxide evolution is also monitored during the CO_2/H_2O conversion. The linear curve fitting indicates the conversion rate of CO_2, which is approximately 50% higher when using CdSe-TiO_2 sample as the photocatalyst. This is likely due to the coupling of pure TiO_2 with CdSe, which extends the adsorption of solar energy in the visible region and generates more electron-hole pairs, due to the smaller band gap of those sensitizers. In all cases, the highest gas yields are recorded when samples are exposed in sunlight at temperatures of 35°C after prolonged sun illumination exposure.

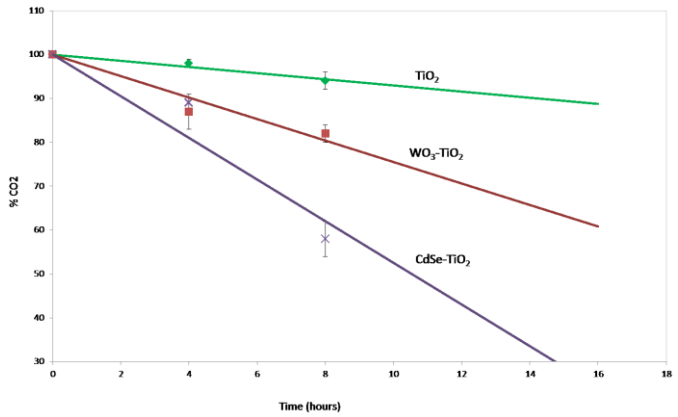

Figure 10. CO_2 reduction process with TiO_2, WO_3-TiO_2 or CdSe-TiO_2 nanophotocatalysts after prolonged exposure in sun light.

Conclusions

We demonstrate solar conversion of carbon dioxide and water vapor to carbon monoxide, hydrogen and hydrocarbons by exposure of titania-based nanophotocatlysts under ambient light only. The photocatalytic performance of the nanoarchitectures developed here was highly dependent upon nanoparticle's shape, morphology, composition, crystallinity, solar activity, and illumination. TiO_2 and WO_3-core TiO_2-shell nanorod arrays fabricated by glancing angle deposition are functionalized with quantum dots (CdSe) prepared by solution chemistry. These nanocomposite structures are used as the photocatalysts for CO_2 conversion under sunlight illumination. A gas chromatographic analysis shows that the primary products are carbon monoxide, hydrogen and hydrocarbons (methanol and methane) after several hours of exposure to sun light. The overall CO_2 conversion efficiency of such core-shell and quantum dot-titania nanostructures is significantly higher than that of pure TiO_2 nanorod array photocatalyst. The improved conversion efficiency may result from the additional absorbance of visible light by WO_3 and CdSe quantum dots and the charge separation at the WO_3-TiO_2 and CdSe-TiO_2 interfaces. The conversion efficiency of such an artificial photosynthesis process remains to be improved for practical applications.

Acknowledgement. The authors would like to acknowledge DOE-Laboratory Directed Research and Development Program for providing funding for this work. They would also like to recognize the contributions of summer intern Rebecca Lewis.

[i] Jing, L. Q. *Solar Energy Materials and Solar Cells* **2003,** 79, 133; (b) Hattori, T. et al. *Materials Transactions* **2006,** *47*, 868; (c) Wang, C.et al. *J. Phys. Chem. Lett*. **2010**, *1*, 48.; (d) Centi, G. et al. *Catalysis Today* **2009**, *148*, 191; (e) Varghese, O.K. et al. *Nano Lett.,* **2009**, *9*, 731; (f) Roy, S.C. et al *ACS Nano* **2010**, *4* ,1259.

[ii] (a) He, Y.; Basnet, P.; Hunyadi Murph, S.E.; Zhao, Y *ACS Applied Materials & Interfaces* **2013,** 5*(22),* 11818-11827.

[iii] (a) Smith, W.; Zhao, Y.-P. *Cat. Comm.* **2009,** 10, 1117; (b) Smith, W.; Zhao, Y. P. *J. Phys. Chem. C* **2008,** *112*, 19635.

[iv] Smith, W.; Zhang, Z. Y.; Zhao, Y. P. *J. Vacuum Science & Technology B* **2007,** *25*, 1875.

[v] Wang, Y.; Tang, Z.; Correa-Duarte,M.A.; Pastoriza-Santos, I. et al. Liz-Marzan, L.M. *J. Phys. Chem. B* **2004,** *108,* 15461-15469.

[vi] Mahtab, R.; Sealey, S.M.; Hunyadi, S.E., Kinard, B.; Ray, T.; Murphy, C.J., *J. Inorg. Biochem.*, **2007**, *101*, 559.

[vii] Tu , W.; Zhou , Y.; Zou, Z. *Adv. Mater.* **2014**, 26, 4607.

[viii] Somnath C. Roy,† Oomman K. Varghese,† Maggie Paulose, and Craig A. Grimes* ACS Nano VOL. 4 ▪ NO. 3 ▪ 1259–1278 ▪ 2010

[ix] Yu, K. P.; Yu, W. Y.; Ku, M. C.; Liou, Y. C.; Chien, S. H. *Appl. Catal., B* **2008**, 84, 112.

[x] Varghese, O. K.; Paulose, M.; LaTempa, T. J.; Grimes, C. *Nano Lett.* **2009**, 9, 731.

[xi] Inoue, T.; Fujishima, A.; Konishi, S.; Honda, K. *Nature,* **1979**, 277, 637.

[xii] Zhang , C. L.; Zhang , Q. Y.; Kang , S. Fat al , *Solid State Lett.* **2013** , 2 , M49 .